

Laser printing of optically resonant hollow crystalline carbon nanostructures from 1D and 2D metal-organic frameworks

Leila R. Mingabudinova,^{a†□} Anastasiia S. Zalogina,^{b†□} Andrei A. Krasilin,^b Margarita I.

Petrova,^b Pavel Trofimov,^b Yuri A. Mezenov,^b Evgeniy V. Ubyivovk,^c Peter Lönnecke,^d

Alexandre Nominé,^b Jaafar Ghanbaja,^e Thierry Belmonte,^e Valentin A. Milichko^{b*}

^aPhysics and Chemistry of Nanostructures group, Ghent University, B-9000 Gent, Belgium

^bDepartment of Nanophotonics and Metamaterials, ITMO University, St. Petersburg, 197101, Russia

^cSt. Petersburg State University, St. Petersburg 199034, Russia

^dInstitut für Anorganische Chemie, Universität Leipzig, 04103, Leipzig, Germany.

^eUniversité de Lorraine, Institut Jean Lamour, UMR CNRS 7198, Nancy F-54011, France

†□These authors contributed equally to this work

*Correspondence to: v.milichko@metalab.ifmo.ru

Synthesis

Synthesis of bulk MOFs. All reagents 1,2-di(4-pyridyl) ethylene (BPE, 97%), Cu(NO₃)₂•6(H₂O) (98%), 4,4'-dipyridyl (98%), dimethyl formamide (DMF, ≥99.8%) were purchased from Sigma-Aldrich and used as received without additional purification. Synthesis of compound **1** was carried out as follows. First, separate solutions of 0.1455 g of Cu(NO₃)₂•6(H₂O) in 2 mL DMF, and 0.094 g of BPE ligand in 1 mL DMF solvent were prepared. Next, the copper nitrate solution was placed into lower vessel, while the ligand solution was placed into an upper vessel of slow diffusion condition device. The synthesis process was initiated by placing a hot glass sphere (heated at 180° for 2 h) into the upper vessel. After the precipitate was formed, the synthesis was continued for 12 h. The procedure yielded blue crystals which were isolated after washing the precipitate 3 times with isopropanol. A similar synthesis procedure was employed for compound **2**, except that the ligand solution was prepared by adding 0.078 g 4,4'-dipyridyl to 1 mL DMF.

Single crystal X-ray diffraction structure analysis. The crystals of the compound **1** and **2** were mounted on goniometer of a Bruker Smart APEX II CCD diffractometer. Measurements were performed at 293 K using graphite-monochromated MoKa radiation ($\lambda = 0.71073 \text{ \AA}$). The data integration and reduction were carried out with SAINT-plus software. For each data set, empirical absorption correction was applied to the collected reflections with SADABS, and the space group was determined using XPREP. The structure was solved by the direct methods using SHELXTL-97 and refined on F2 by full-matrix least-squares using the SHELXL-97 program package. All non-hydrogen atoms were refined anisotropically. Hydrogen atoms were placed in calculated positions and included as riding atoms with isotropic displacement parameters 1.2–1.5 times Ueq of the attached C atoms. All structures were examined using the Addsym subroutine of PLATON to ensure that no additional symmetry could be applied to the models.

Table S1. Crystal data and structure refinement for Cu-based MOF (**1**).

Empirical formula	C ₁₈ H ₂₅ CuN ₅ O ₈					
Formula weight	502.97					
Temperature	130(2) K					
Wavelength	71.073 pm					
Crystal system	Triclinic					
Space group	P -1					
Unit cell dimensions	a = 925.42(4) pm	α = 66.490(4)°.	b = 1027.60(5) pm	β = 85.829(4)°.	c = 1263.02(5) pm	γ = 85.602(4)°.
Volume	1.09697(9) nm ³					
Z	2					
Density (calculated)	1.523 Mg/m ³					
Absorption coefficient	1.050 mm ⁻¹					
F(000)	522					
Crystal size	0.20 x 0.05 x 0.05 mm ³					
Theta range for data collection	2.164 to 29.263°.					
Index ranges	-12≤h≤12, -11≤k≤13, -17≤l≤17					

Reflections collected	10740
Independent reflections	5033 [R(int) = 0.0409]
Completeness to theta = 26.375°	100.0 %
Absorption correction	Semi-empirical from equivalents
Max. and min. transmission	1.00000 and 0.99120
Refinement method	Full-matrix least-squares on F ²
Data / restraints / parameters	5033 / 8 / 294
Goodness-of-fit on F ²	1.033
Final R indices [I>2sigma(I)]	R1 = 0.0629, wR2 = 0.1534
R indices (all data)	R1 = 0.1000, wR2 = 0.1757
Largest diff. peak and hole	0.604 and -0.622 e.Å ⁻³

Comments: Structure solution with SHELXT-2014 (dual-space method). Anisotropic refinement of all non-hydrogen atoms, except disordered parts of the structure, with SHELXL-2016. All hydrogen atoms were calculated on idealized positions. The propanol solvent molecule (O8, C16 to C18) was found to be disordered over two positions with a ratio 0.684(8) : 0.316(8). Chains are formed in (1-10) direction (Fig. S1). Copper is coordinated in a square pyramidal fashion with one elongated Cu1-O1' bond (Fig. S2). The formulae of the compound is [Cu(C₁₂H₁₀N₂)(NO₃)₂]•DMF•i-PrOH.

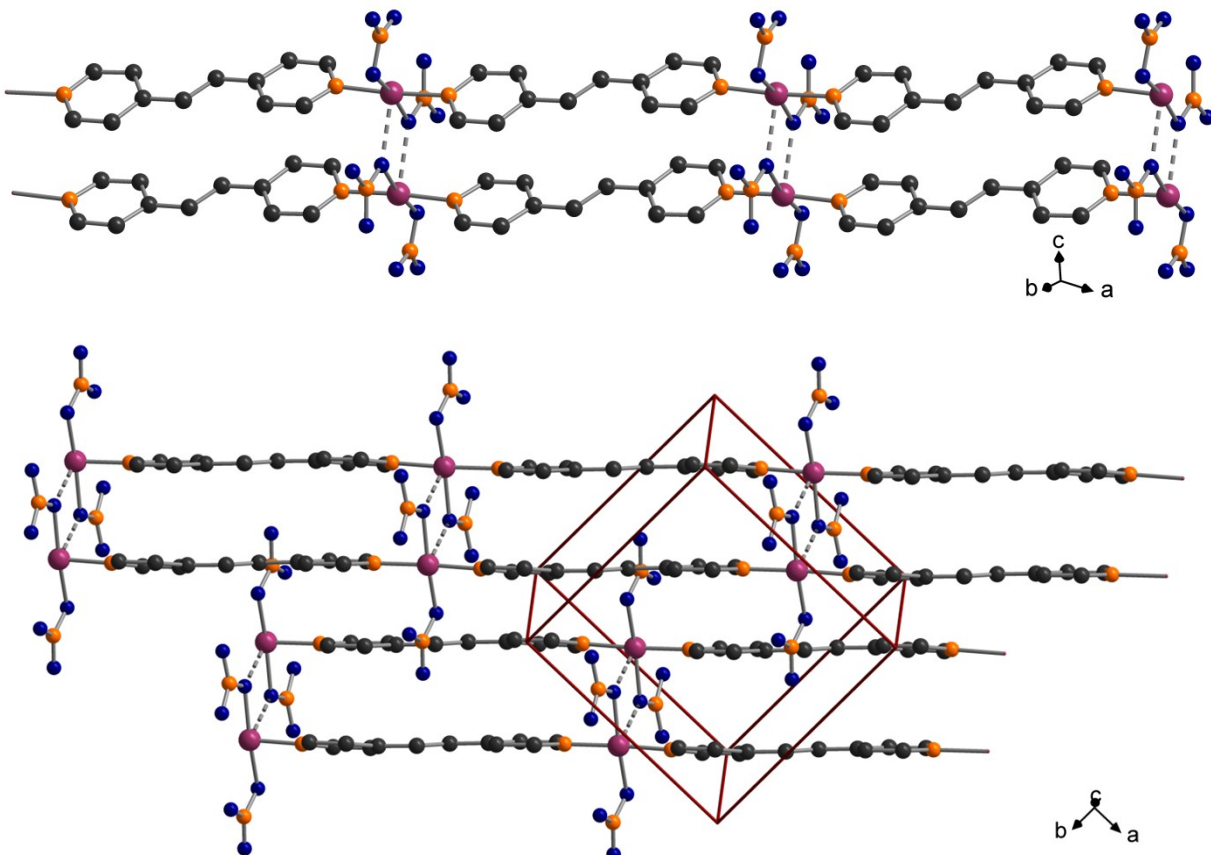


Fig. S1. Chains in (1-10) direction for **1** (bottom: Two of them passing the unit cell). Orange – Nitrogen, Navy – Oxygen, Violet – Copper, Black – Carbon.

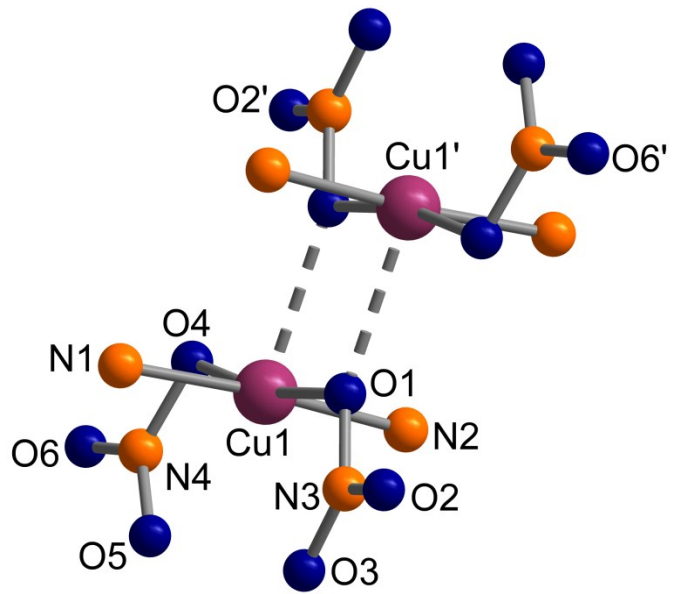


Fig. S2. SBU and coordination sphere at copper for **1**.

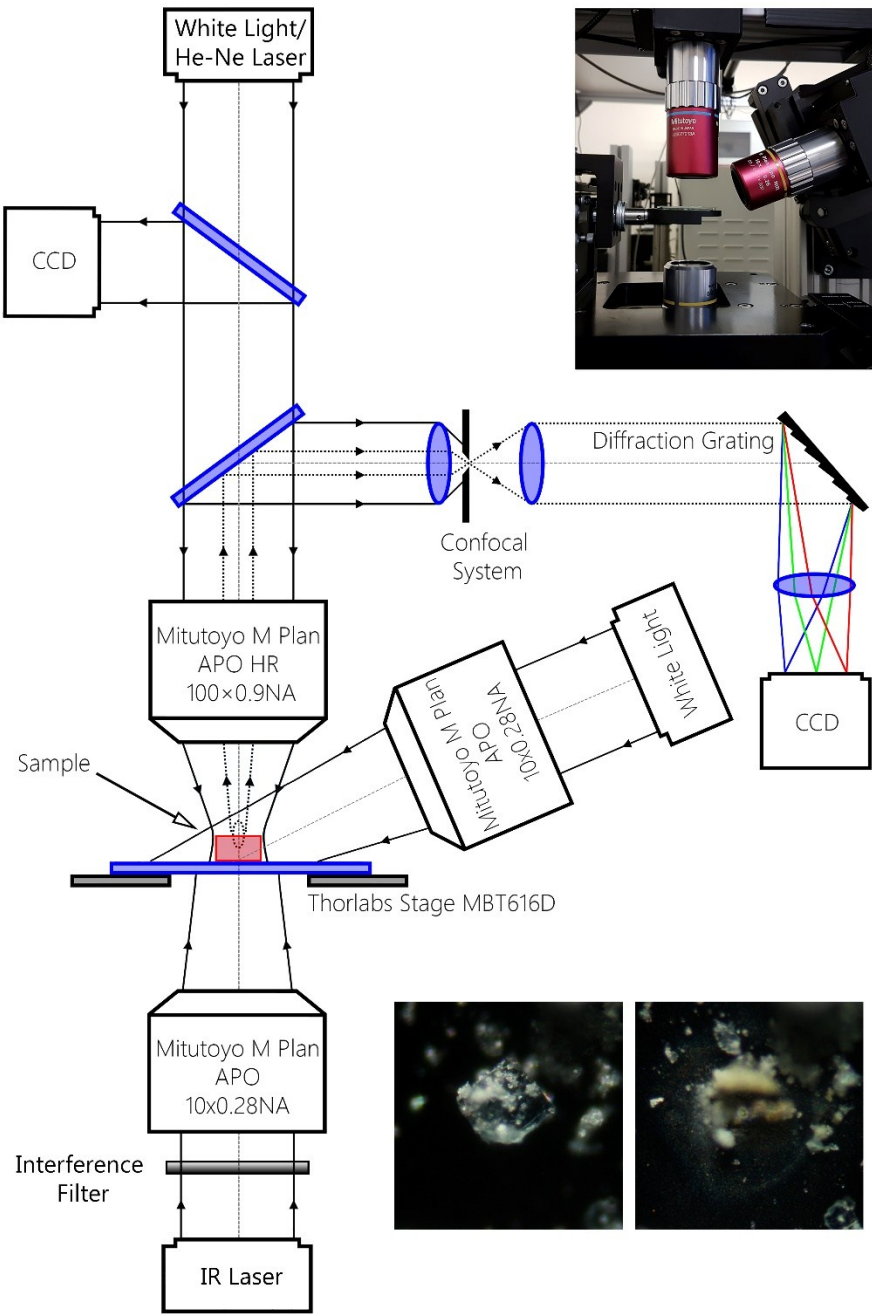


Fig. S3. Scheme of laser-assisted fabrication of c-HCS: IR laser source (Avesta Project, 150 fs, 1050 nm, 80 MHz repetition rate) is used to irradiate single MOF crystals on air placed on silica substrate and motorized stage. The interference filter placed between the laser source and an objective (Mitutoyo M Plan APO 10x 0.28 NA) is used to vary the power from 60 to 160 mW. The upper objective (Mitutoyo M Plan APO 10x 0.28 NA) is used to irradiate the single MOF crystals and fabricated c-HCS at the 67° to the surface normal by white light. Other objective (Mitutoyo M Plan APO HR 100x 0.9 NA) is used to visualize the process and collect the optical signal from single c-HCS for spectral analysis by confocal spectrometer Horiba LabRam with a cooled CCD camera Andor DU 420A-OE 325 and 600 g/mm diffraction grating (see Fig. S16).

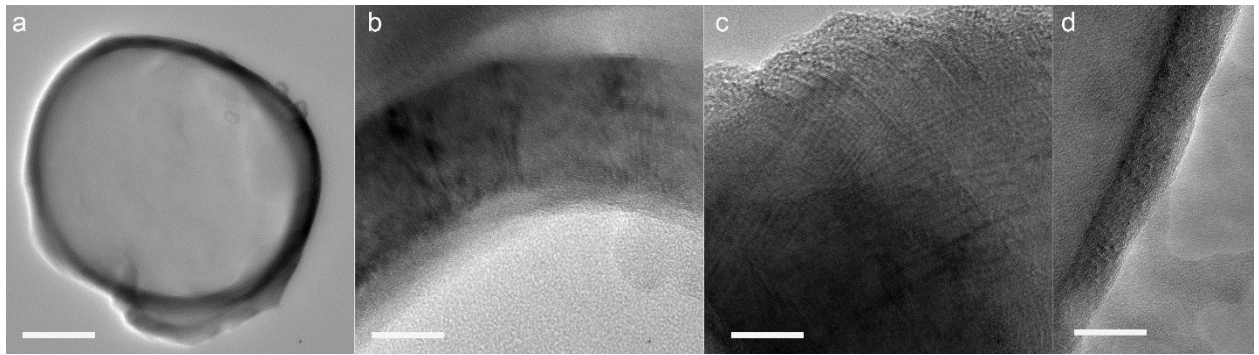


Fig. S4. TEM image of c-HCS obtained from **1** (**a**), and zoomed shell (**b-d**). The interlayer period is $3.2 \pm 0.1 \text{ \AA}$. Scale bars, 100 nm, 20 nm, 10 nm, 20 nm, respectively.

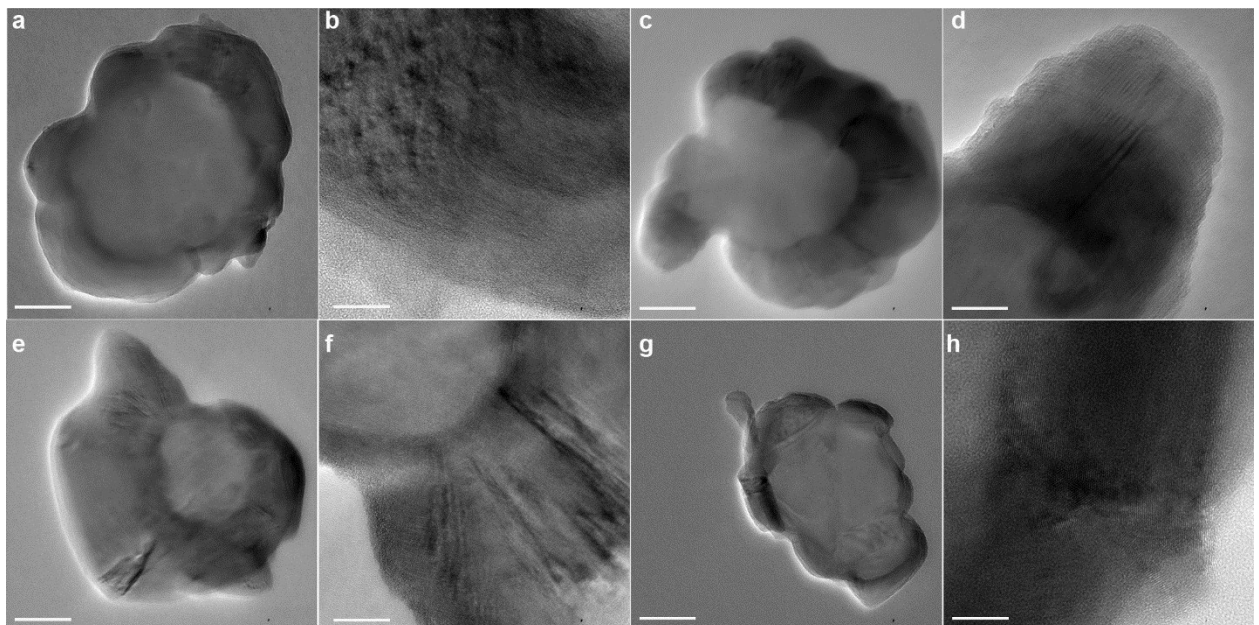
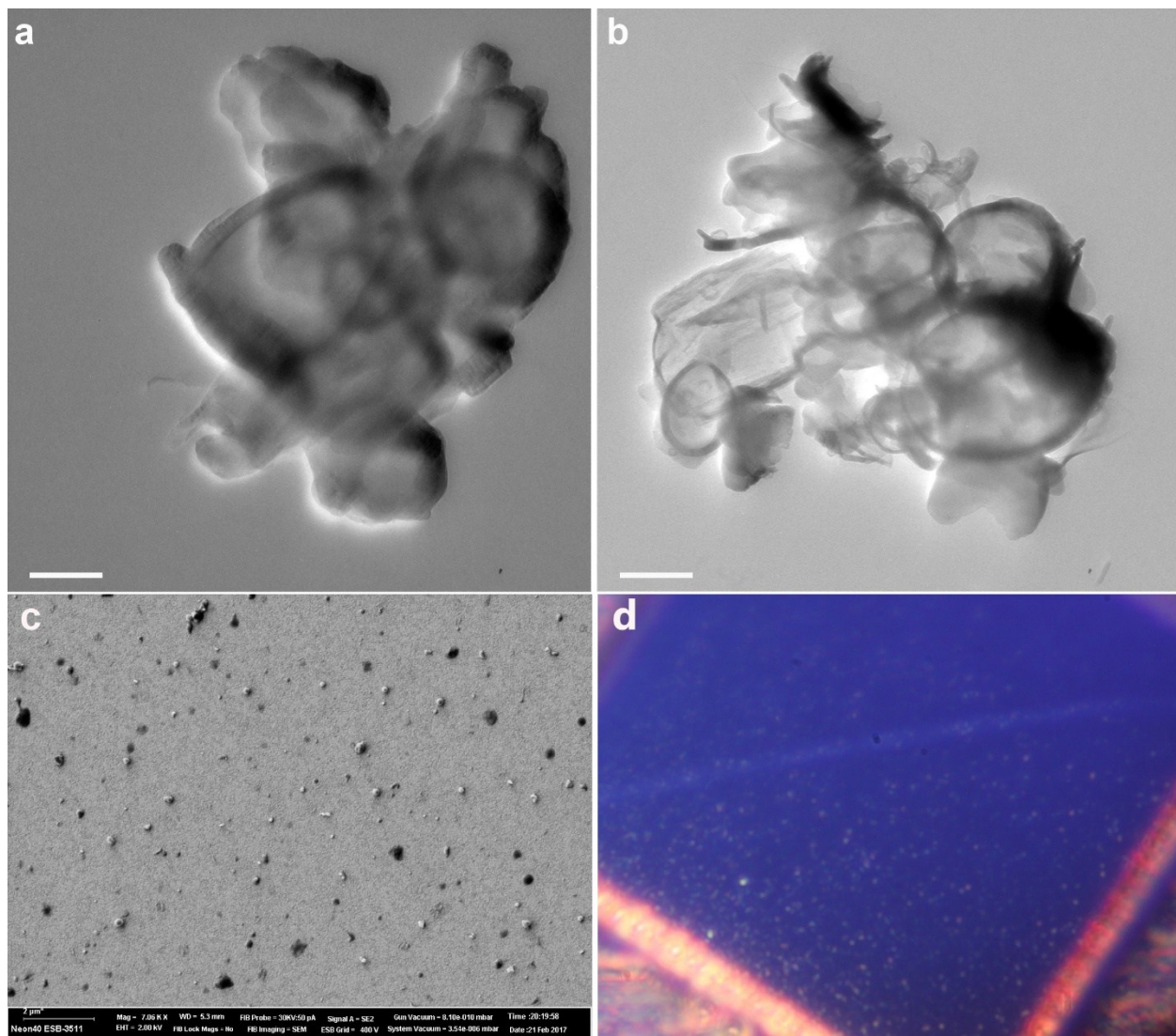


Fig. S5. TEM images of c-HCSs obtained from **1** with different diameters. **a,b**, c-HCS with a size of $\sim 350 \text{ nm}$ and shell thickness of 50-100 nm. Scale bar, 100 and 20 nm. **c,d**, c-HCS with a size of $\sim 330 \text{ nm}$ and shell thickness of 50-130 nm. Scale bar, 100 and 20 nm. **e,f**, c-HCS with a size of $\sim 300 \text{ nm}$ and shell thickness of 50-100 nm. Scale bars, 50 and 20 nm. **g,h**, c-HCS with a size of $\sim 250 \text{ nm}$ and shell thickness of 20-50 nm. Scale bars, 100 and 10 nm.



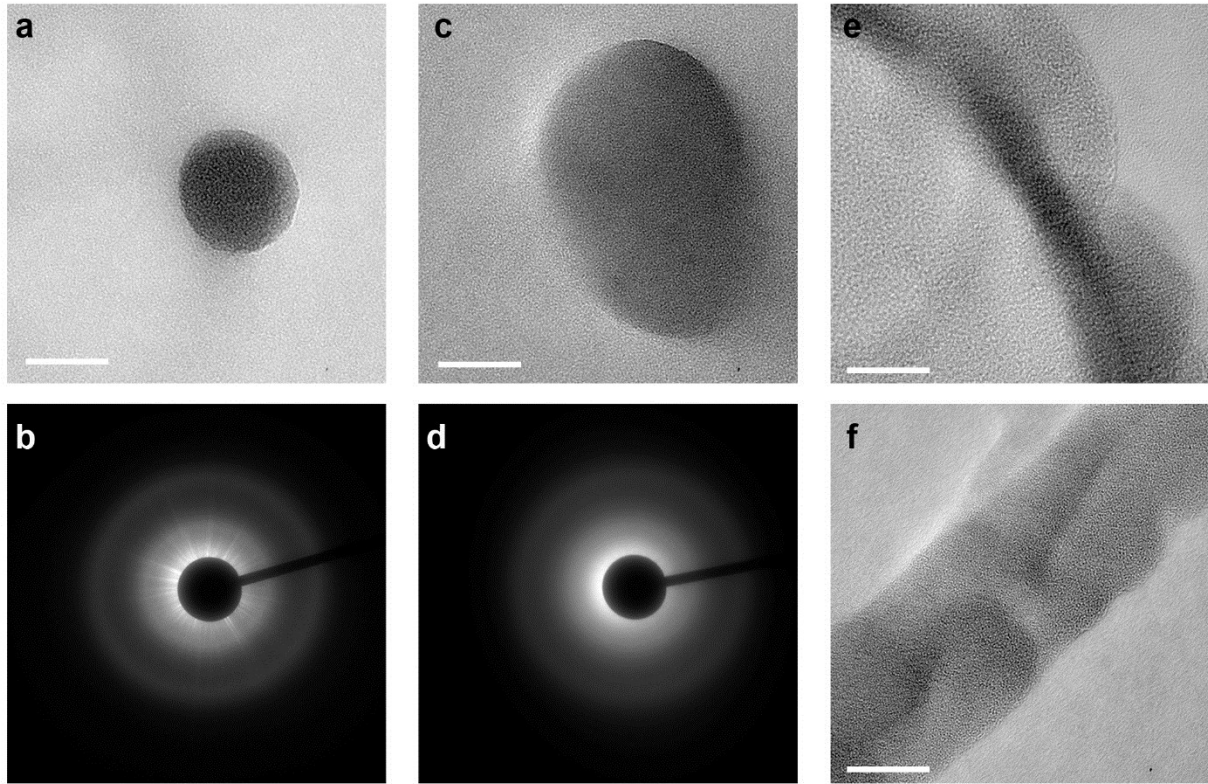


Fig. S7. TEM images of the 20-80 nm nanoparticles obtained from **1**. **a,b**, 25-nm amorphous nanoparticle with its electron diffraction. Scale bar, 20 nm. **c,d**, 60-nm amorphous nanoparticle with its electron diffraction. Scale bar, 20 nm. **e,f**, TEM images of the border of amorphous nanoparticle from **c**. Scale bar, 15 nm.

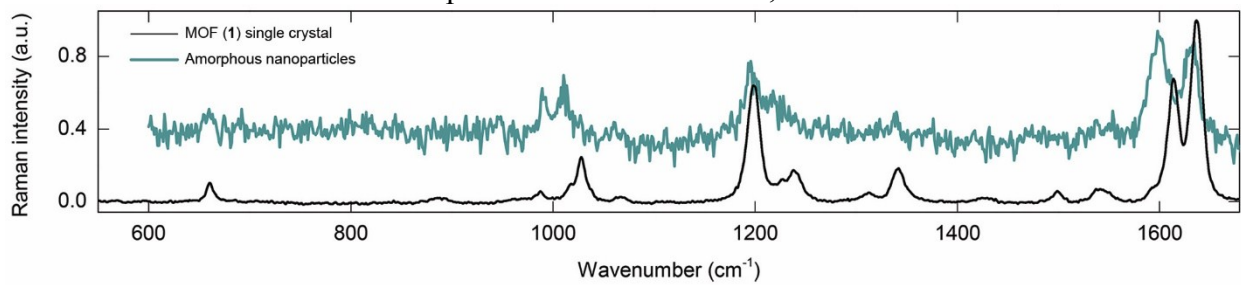


Fig. S8. Raman spectrum for the MOF (**1**) and amorphous nanoparticles (Fig. S7). The broadening corresponded to ring deformation, breathing and C-N bending, was an indicator of formation the structural defects such as dislocations and stacking faults. The red shift of the Raman peaks especially for C-C, C-N, C=C, and C-H bonds evidenced a decrease in the vibration energy due to the bond softening or stretching.

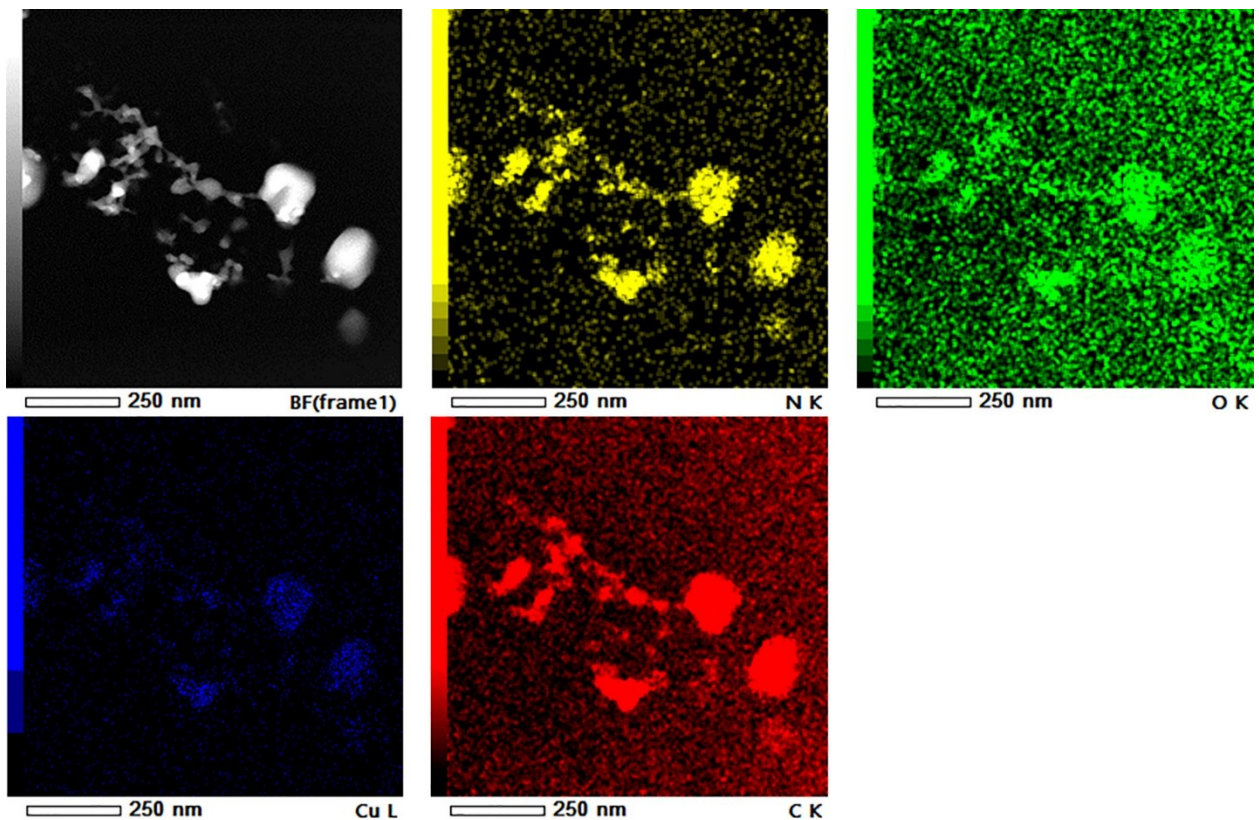


Fig. S9. EDX analysis of the amorphous nanoparticles (Fig. S7).

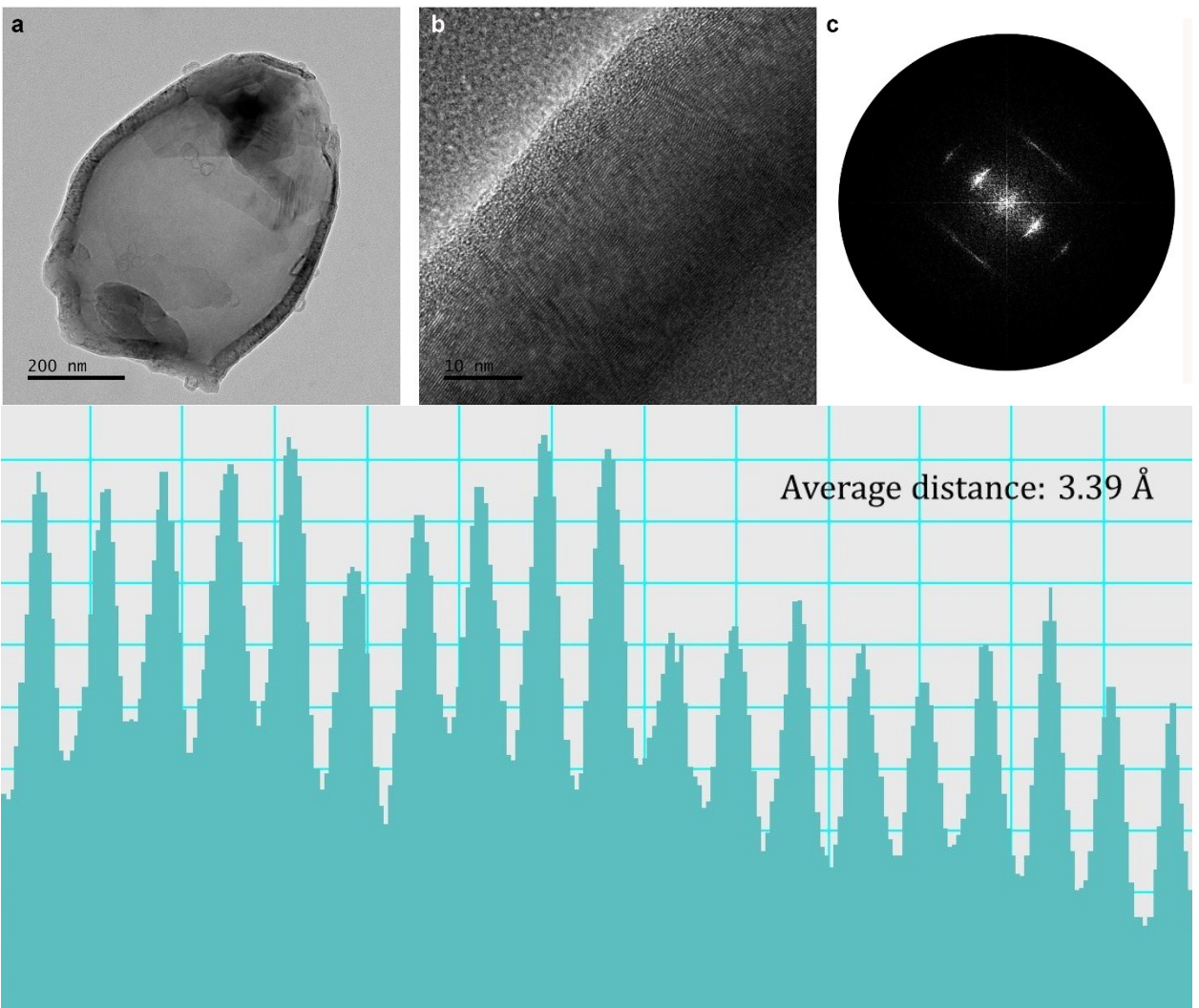


Fig. S10. TEM images (**a,b**) of c-HCS obtained from **1**. (**c**) FFT analysis of the interplanar distance, $d_{hkl} = 3.39 \pm 0.10 \text{ \AA}$. Bottom – profile of the TEM image (**b**) demonstrating the average distance between layers, 3.39 \AA .

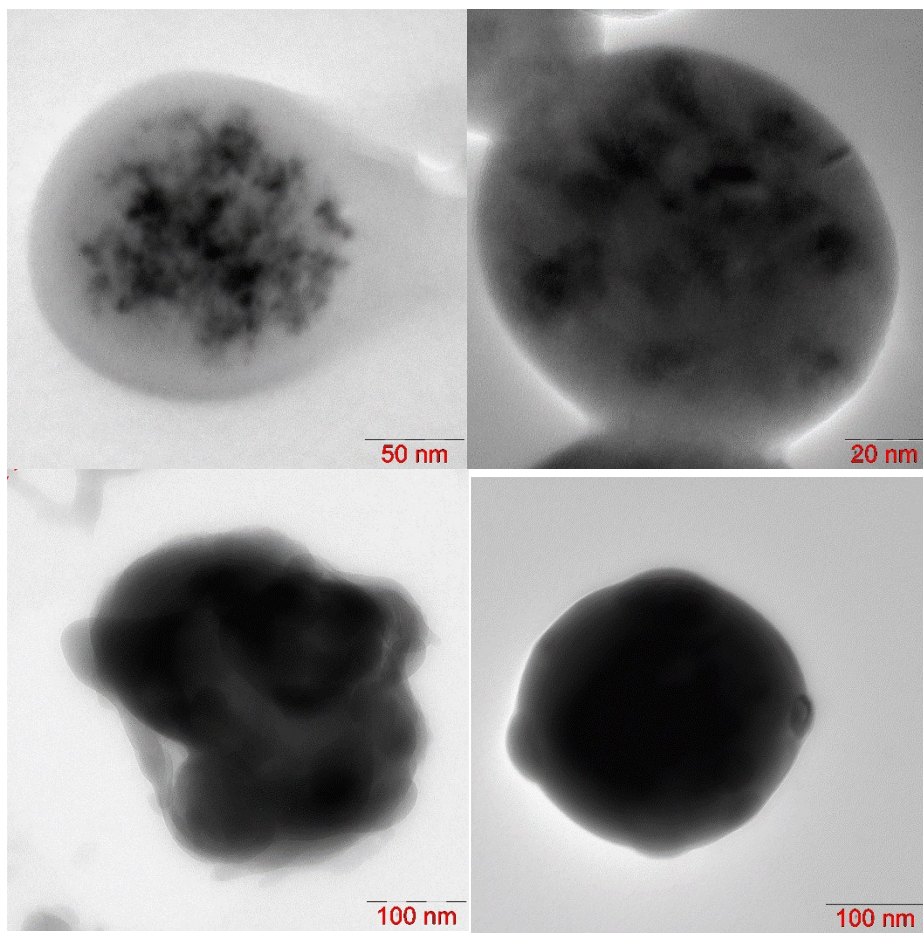


Fig. S11. TEM images of nanostructures demonstrating nanometer scale inclusions with high electronic density. The nanostructures were obtained from **1** (left, top and bottom) and **2** (right, top and bottom).

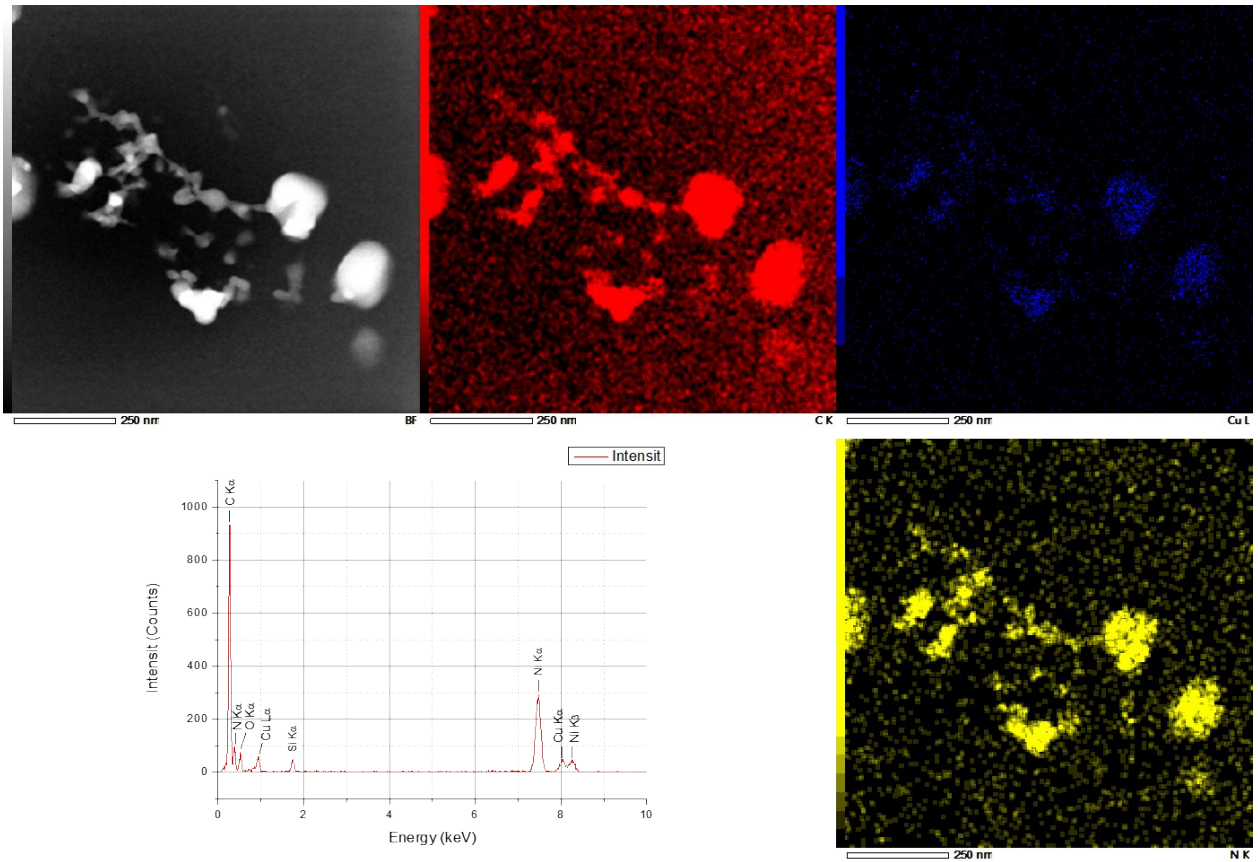


Fig. S12. EDX map of the nanostructures from Fig. S11 demonstrating the presence of Copper (Red colour) inside the printed nanostructures.

Table S2. Crystal data and structure refinement for Cu-based MOF with BPY ligand (**2**).

Empirical formula	C32 H44 Cu N10 O10
Formula weight	792.31
Temperature	130(2) K
Wavelength	71.073 pm
Crystal system	Monoclinic
Space group	P 21/n
Unit cell dimensions	$a = 1559.44(3)$ pm $\alpha = 90^\circ$. $b = 1526.43(3)$ pm $\beta = 90.224(2)^\circ$. $c = 1577.61(4)$ pm $\gamma = 90^\circ$.
Volume	3.75528(14) nm ³
Z	4
Density (calculated)	1.401 Mg/m ³
Absorption coefficient	0.649 mm ⁻¹
F(000)	1660
Crystal size	0.4 x 0.3 x 0.03 mm ³
Theta range for data collection	2.267 to 30.517°.
Index ranges	-22<=h<=21, -20<=k<=21, -18<=l<=22
Reflections collected	36943
Independent reflections	10516 [R(int) = 0.0524]
Completeness to theta = 28.285°	99.9 %
Absorption correction	Semi-empirical from equivalents
Max. and min. transmission	1 and 0.81877
Refinement method	Full-matrix least-squares on F ²
Data / restraints / parameters	10516 / 0 / 486
Goodness-of-fit on F ²	1.155
Final R indices [I>2sigma(I)]	R1 = 0.0632, wR2 = 0.1511
R indices (all data)	R1 = 0.1042, wR2 = 0.1655
Largest diff. peak and hole	1.278 and -0.706 e.Å ⁻³

Comments: Structure solution with SHELXT-2014 (dual-space method). Anisotropic refinement of all non-hydrogen atoms with SHELXL-2014. All hydrogen atoms were calculated on idealized positions. Coordination polymer with layer structure. The formulae may be given as [Cu(bipy)₂(DMF)(NO₃)] [NO₃] • 3 DMF.

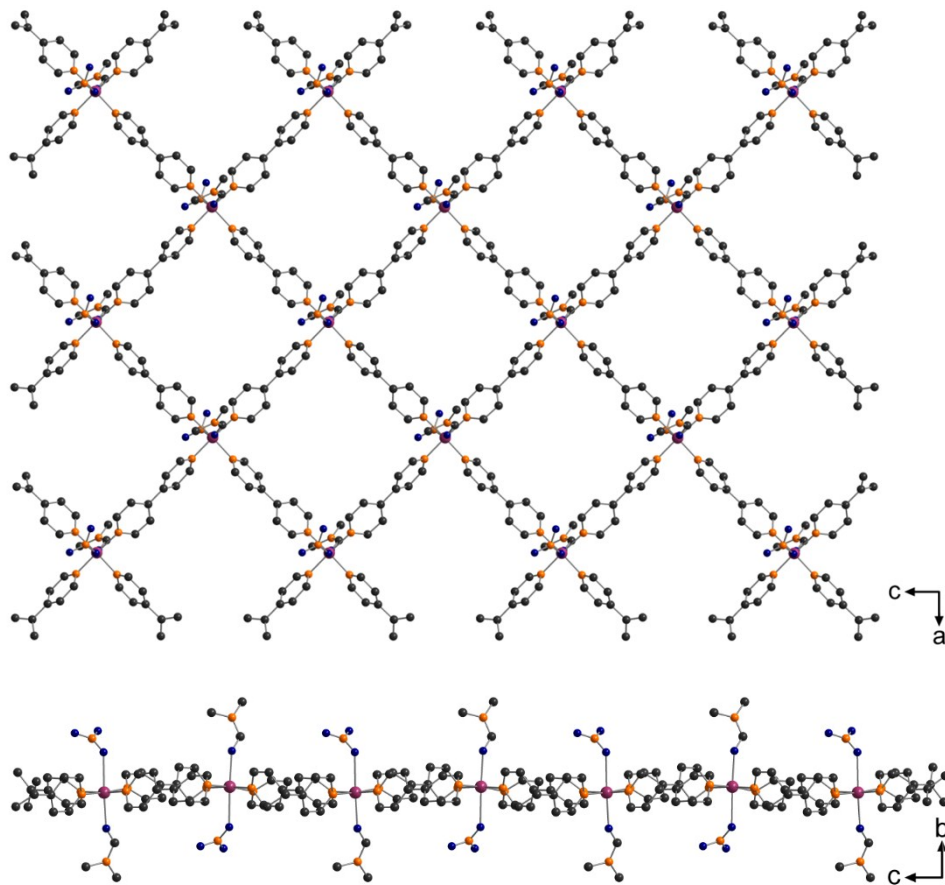


Fig. S13. Layer structure viewing along (010) and (100) for **2**. Non-coordinating moieties (3 DMF and one NO_3^- -anion) had been removed for clarity. Orange – Nitrogen, Navy – Oxygen, Violet – Copper, Black – Carbon.

Table S3. Atomic coordinates ($\times 10^4$) and equivalent isotropic displacement parameters ($\text{pm}^2 \times 10^{-1}$) for **2**. $U(\text{eq})$ is defined as one third of the trace of the orthogonalized U^{ij} tensor.

	x	y	z	$U(\text{eq})$
Cu(1)	2231(1)	7621(1)	5654(1)	14(1)
O(1)	2114(2)	9103(2)	5572(2)	22(1)
O(2)	2861(3)	8117(3)	2505(3)	77(1)
O(3)	1032(2)	5539(3)	-403(2)	54(1)
O(4)	2556(3)	2833(3)	5554(3)	80(1)
O(5)	2248(2)	5952(2)	5677(2)	21(1)
O(6)	2217(2)	5162(2)	6820(2)	32(1)
O(7)	1185(2)	5072(2)	5904(2)	46(1)

O(8)	-143(2)	10190(2)	6608(2)	44(1)
O(9)	-687(2)	10298(2)	7868(2)	42(1)
O(10)	-1412(2)	9689(2)	6867(2)	42(1)
N(1)	3178(2)	7566(2)	4786(2)	15(1)
N(2)	6332(2)	7419(2)	1580(2)	15(1)
N(3)	3155(2)	7694(2)	6548(2)	15(1)
N(4)	6352(2)	7564(2)	9721(2)	14(1)
N(5)	1583(2)	10479(2)	5565(2)	24(1)
N(6)	3259(3)	9212(3)	1613(3)	51(1)
N(7)	1340(3)	6050(3)	924(3)	50(1)
N(8)	3632(3)	3838(3)	5474(3)	50(1)
N(9)	1885(2)	5388(2)	6136(2)	23(1)
N(10)	-742(2)	10061(2)	7112(2)	28(1)
C(1)	3279(2)	6858(2)	4296(2)	20(1)
C(2)	3905(2)	6793(2)	3683(2)	21(1)
C(3)	4461(2)	7492(2)	3560(2)	19(1)
C(4)	4373(2)	8216(2)	4092(2)	21(1)
C(5)	3731(2)	8234(2)	4691(2)	20(1)
C(6)	6431(2)	7950(2)	2251(2)	19(1)
C(7)	5845(2)	7996(2)	2907(2)	20(1)
C(8)	5115(2)	7471(2)	2880(2)	18(1)
C(9)	5013(2)	6929(2)	2178(2)	21(1)
C(10)	5626(2)	6918(2)	1554(2)	19(1)
C(11)	3259(2)	8388(2)	7052(2)	19(1)
C(12)	3895(2)	8424(2)	7673(2)	20(1)
C(13)	4448(2)	7715(2)	7772(2)	16(1)
C(14)	4335(2)	6993(2)	7237(2)	19(1)
C(15)	3688(2)	7013(2)	6642(2)	19(1)
C(16)	6424(2)	7110(2)	8999(2)	17(1)
C(17)	5836(2)	7164(2)	8349(2)	18(1)
C(18)	5126(2)	7702(2)	8434(2)	16(1)
C(19)	5062(2)	8200(2)	9169(2)	20(1)
C(20)	5683(2)	8118(2)	9789(2)	19(1)
C(21)	1950(3)	10688(3)	6382(3)	35(1)
C(22)	1017(3)	11130(3)	5160(3)	33(1)
C(23)	1686(2)	9695(2)	5234(2)	22(1)

C(24)	3845(5)	8688(6)	1151(4)	106(3)
C(25)	3115(8)	10089(5)	1356(5)	129(4)
C(26)	2808(3)	8863(4)	2242(3)	51(1)
C(27)	656(5)	5595(5)	1325(5)	90(3)
C(28)	1920(4)	6571(4)	1458(4)	63(2)
C(29)	1465(3)	5989(4)	99(3)	48(1)
C(30)	3899(6)	3589(6)	4648(4)	111(3)
C(31)	4071(3)	4556(4)	5874(4)	57(2)
C(32)	2977(3)	3432(3)	5851(4)	49(1)

Table S4. Bond lengths [pm] and angles [$^{\circ}$] for **2**.

Cu(1)-N(3)	201.4(3)
Cu(1)-N(1)	201.9(3)
Cu(1)-N(4)#1	202.8(3)
Cu(1)-N(2)#2	203.0(3)
Cu(1)-O(1)	227.4(3)
O(1)-C(23)	124.2(4)
O(2)-C(26)	121.5(7)
O(3)-C(29)	124.5(6)
O(4)-C(32)	121.9(6)
O(5)-N(9)	126.1(4)
O(6)-N(9)	124.5(4)
O(7)-N(9)	124.6(4)
O(8)-N(10)	124.4(4)
O(9)-N(10)	124.9(4)
O(10)-N(10)	124.9(4)
N(1)-C(1)	133.9(4)
N(1)-C(5)	134.5(4)
N(2)-C(10)	134.2(4)
N(2)-C(6)	134.2(4)
N(2)-Cu(1)#3	203.0(3)
N(3)-C(11)	133.5(4)
N(3)-C(15)	134.0(4)
N(4)-C(16)	133.8(4)
N(4)-C(20)	134.7(4)
N(4)-Cu(1)#4	202.8(3)
N(5)-C(23)	131.6(5)
N(5)-C(21)	144.4(5)
N(5)-C(22)	147.3(5)
N(6)-C(26)	133.0(6)
N(6)-C(25)	141.7(8)
N(6)-C(24)	141.8(7)
N(7)-C(29)	132.0(6)
N(7)-C(27)	142.4(7)
N(7)-C(28)	146.7(7)

N(8)-C(32)	133.5(7)
N(8)-C(30)	142.2(8)
N(8)-C(31)	143.8(7)
C(1)-C(2)	138.2(5)
C(2)-C(3)	138.9(5)
C(3)-C(4)	139.4(5)
C(3)-C(8)	148.4(4)
C(4)-C(5)	137.9(5)
C(6)-C(7)	138.5(5)
C(7)-C(8)	139.3(5)
C(8)-C(9)	139.0(5)
C(9)-C(10)	137.5(5)
C(11)-C(12)	139.2(5)
C(12)-C(13)	139.3(5)
C(13)-C(14)	139.8(5)
C(13)-C(18)	148.3(4)
C(14)-C(15)	137.5(5)
C(16)-C(17)	137.6(4)
C(17)-C(18)	138.5(5)
C(18)-C(19)	139.1(5)
C(19)-C(20)	137.9(5)
N(3)-Cu(1)-N(1)	87.40(11)
N(3)-Cu(1)-N(4)#1	174.49(12)
N(1)-Cu(1)-N(4)#1	89.78(11)
N(3)-Cu(1)-N(2)#2	89.52(11)
N(1)-Cu(1)-N(2)#2	174.70(11)
N(4)#1-Cu(1)-N(2)#2	92.93(10)
N(3)-Cu(1)-O(1)	92.42(10)
N(1)-Cu(1)-O(1)	93.55(10)
N(4)#1-Cu(1)-O(1)	92.48(10)
N(2)#2-Cu(1)-O(1)	90.87(10)
C(23)-O(1)-Cu(1)	142.2(2)
C(1)-N(1)-C(5)	118.1(3)
C(1)-N(1)-Cu(1)	120.9(2)
C(5)-N(1)-Cu(1)	121.0(2)
C(10)-N(2)-C(6)	117.4(3)

C(10)-N(2)-Cu(1)#3	122.0(2)
C(6)-N(2)-Cu(1)#3	120.6(2)
C(11)-N(3)-C(15)	118.4(3)
C(11)-N(3)-Cu(1)	123.1(2)
C(15)-N(3)-Cu(1)	118.5(2)
C(16)-N(4)-C(20)	117.4(3)
C(16)-N(4)-Cu(1)#4	119.1(2)
C(20)-N(4)-Cu(1)#4	123.5(2)
C(23)-N(5)-C(21)	120.5(3)
C(23)-N(5)-C(22)	121.0(3)
C(21)-N(5)-C(22)	118.2(3)
C(26)-N(6)-C(25)	120.5(5)
C(26)-N(6)-C(24)	120.1(5)
C(25)-N(6)-C(24)	119.2(6)
C(29)-N(7)-C(27)	121.2(5)
C(29)-N(7)-C(28)	120.8(5)
C(27)-N(7)-C(28)	118.0(5)
C(32)-N(8)-C(30)	120.8(5)
C(32)-N(8)-C(31)	121.5(5)
C(30)-N(8)-C(31)	117.7(5)
O(6)-N(9)-O(7)	120.6(3)
O(6)-N(9)-O(5)	120.0(3)
O(7)-N(9)-O(5)	119.4(3)
O(8)-N(10)-O(10)	120.2(4)
O(8)-N(10)-O(9)	121.0(3)
O(10)-N(10)-O(9)	118.7(4)
N(1)-C(1)-C(2)	123.2(3)
C(1)-C(2)-C(3)	119.1(3)
C(2)-C(3)-C(4)	117.5(3)
C(2)-C(3)-C(8)	121.0(3)
C(4)-C(3)-C(8)	121.6(3)
C(5)-C(4)-C(3)	120.2(3)
N(1)-C(5)-C(4)	121.9(3)
N(2)-C(6)-C(7)	123.1(3)
C(6)-C(7)-C(8)	119.3(3)
C(9)-C(8)-C(7)	117.3(3)

C(9)-C(8)-C(3)	120.8(3)
C(7)-C(8)-C(3)	121.9(3)
C(10)-C(9)-C(8)	120.0(3)
N(2)-C(10)-C(9)	122.9(3)
N(3)-C(11)-C(12)	122.4(3)
C(11)-C(12)-C(13)	119.1(3)
C(12)-C(13)-C(14)	117.9(3)
C(12)-C(13)-C(18)	122.0(3)
C(14)-C(13)-C(18)	120.1(3)
C(15)-C(14)-C(13)	119.0(3)
N(3)-C(15)-C(14)	123.1(3)
N(4)-C(16)-C(17)	123.0(3)
C(16)-C(17)-C(18)	119.7(3)
C(17)-C(18)-C(19)	117.6(3)
C(17)-C(18)-C(13)	120.6(3)
C(19)-C(18)-C(13)	121.8(3)
C(20)-C(19)-C(18)	119.3(3)
N(4)-C(20)-C(19)	122.9(3)
O(1)-C(23)-N(5)	123.8(3)
O(2)-C(26)-N(6)	126.5(5)
O(3)-C(29)-N(7)	125.8(5)
O(4)-C(32)-N(8)	126.1(6)

Symmetry transformations used to generate equivalent atoms:

#1 x-1/2,-y+3/2,z-1/2 #2 x-1/2,-y+3/2,z+1/2
#3 x+1/2,-y+3/2,z-1/2 #4 x+1/2,-y+3/2,z+1/2

Table S5. Anisotropic displacement parameters ($\text{pm}^2 \times 10^{-1}$) for **2**. The anisotropic displacement factor exponent takes the form: $-2\pi^2 [h^2 a^* a^* U_{11} + \dots + 2 h k a^* b^* U_{12}]$

	U ₁₁	U ₂₂	U ₃₃	U ₂₃	U ₁₃	U ₁₂
Cu(1)	9(1)	24(1)	8(1)	0(1)	1(1)	0(1)
O(1)	20(1)	23(1)	21(1)	-1(1)	1(1)	0(1)
O(2)	92(3)	76(3)	64(3)	25(2)	-7(2)	-24(3)
O(3)	47(2)	68(3)	48(2)	0(2)	-1(2)	17(2)
O(4)	98(4)	59(3)	81(3)	-11(2)	2(3)	-31(2)
O(5)	21(1)	26(1)	17(1)	5(1)	3(1)	-5(1)
O(6)	42(2)	33(2)	22(1)	7(1)	-8(1)	0(1)
O(7)	35(2)	51(2)	53(2)	24(2)	-17(2)	-24(2)
O(8)	43(2)	42(2)	47(2)	0(2)	15(2)	-8(2)
O(9)	61(2)	39(2)	26(2)	3(1)	-7(1)	-14(2)
O(10)	31(2)	52(2)	44(2)	-8(2)	-5(1)	-4(1)
N(1)	12(1)	23(2)	11(1)	1(1)	2(1)	0(1)
N(2)	12(1)	22(2)	11(1)	0(1)	1(1)	-1(1)
N(3)	11(1)	23(2)	12(1)	1(1)	0(1)	0(1)
N(4)	10(1)	20(2)	12(1)	-1(1)	1(1)	2(1)
N(5)	30(2)	23(2)	19(2)	0(1)	-1(1)	3(1)
N(6)	61(3)	58(3)	34(2)	19(2)	14(2)	22(2)
N(7)	54(3)	51(3)	45(3)	-1(2)	5(2)	9(2)
N(8)	63(3)	42(2)	44(3)	7(2)	-1(2)	-6(2)
N(9)	22(2)	23(2)	23(2)	3(1)	-2(1)	-1(1)
N(10)	32(2)	21(2)	31(2)	5(1)	-2(1)	0(1)
C(1)	18(2)	23(2)	20(2)	0(1)	4(1)	-2(1)
C(2)	19(2)	24(2)	19(2)	-1(1)	6(1)	-2(1)
C(3)	15(1)	25(2)	16(2)	-1(1)	4(1)	0(1)
C(4)	17(2)	26(2)	21(2)	-2(2)	6(1)	-5(1)
C(5)	17(2)	25(2)	17(2)	-6(1)	2(1)	-2(1)
C(6)	15(2)	26(2)	14(2)	-1(1)	2(1)	-4(1)
C(7)	19(2)	26(2)	16(2)	-6(1)	3(1)	-4(1)
C(8)	14(1)	25(2)	14(2)	1(1)	4(1)	-1(1)
C(9)	16(2)	27(2)	20(2)	-1(2)	4(1)	-3(1)
C(10)	18(2)	26(2)	13(2)	-4(1)	1(1)	-3(1)

C(11)	17(2)	22(2)	17(2)	0(1)	-2(1)	4(1)
C(12)	20(2)	22(2)	18(2)	-5(1)	-6(1)	4(1)
C(13)	13(1)	22(2)	13(2)	3(1)	-1(1)	0(1)
C(14)	17(2)	21(2)	18(2)	1(1)	-2(1)	3(1)
C(15)	18(2)	21(2)	18(2)	-2(1)	-3(1)	1(1)
C(16)	13(1)	23(2)	15(2)	0(1)	-1(1)	2(1)
C(17)	17(2)	23(2)	14(2)	-3(1)	-1(1)	1(1)
C(18)	13(1)	22(2)	14(2)	2(1)	-3(1)	-2(1)
C(19)	17(2)	24(2)	20(2)	-3(1)	-2(1)	4(1)
C(20)	16(2)	25(2)	15(2)	-4(1)	0(1)	2(1)
C(21)	44(2)	34(2)	26(2)	-7(2)	-5(2)	4(2)
C(22)	41(2)	27(2)	30(2)	2(2)	-2(2)	12(2)
C(23)	21(2)	23(2)	20(2)	-1(2)	1(1)	1(1)
C(24)	94(5)	162(8)	62(4)	41(5)	43(4)	84(6)
C(25)	244(12)	76(5)	68(5)	38(4)	43(6)	52(7)
C(26)	36(3)	74(4)	44(3)	13(3)	4(2)	13(2)
C(27)	118(6)	78(5)	75(5)	-18(4)	52(5)	-35(4)
C(28)	66(4)	66(4)	58(4)	-14(3)	-7(3)	10(3)
C(29)	35(3)	67(4)	43(3)	2(3)	1(2)	14(2)
C(30)	173(9)	117(7)	44(4)	-15(4)	25(5)	-67(6)
C(31)	44(3)	47(3)	80(4)	-11(3)	0(3)	1(2)
C(32)	56(3)	34(3)	58(3)	5(2)	6(3)	4(2)

Table S6. Hydrogen coordinates ($\times 10^4$) and isotropic displacement parameters ($\text{pm}^2 \times 10^{-1}$) for **2**.

	x	y	z	U(eq)
H(1)	2901	6376	4374	24
H(2)	3956	6277	3350	25
H(4)	4755	8697	4042	25
H(5)	3679	8734	5047	23
H(6)	6926	8312	2277	22
H(7)	5940	8381	3371	24
H(9)	4520	6566	2130	25
H(10)	5546	6538	1083	23
H(11)	2887	8876	6984	23
H(12)	3950	8926	8025	24
H(14)	4699	6497	7285	22
H(15)	3617	6520	6281	22
H(16)	6904	6733	8933	20
H(17)	5917	6835	7845	22
H(19)	4596	8593	9244	24
H(20)	5638	8468	10285	22
H(21A)	1558	10500	6831	52
H(21B)	2041	11322	6422	52
H(21C)	2500	10385	6448	52
H(22A)	845	10919	4598	49
H(22B)	1324	11687	5104	49
H(22C)	506	11215	5510	49
H(23)	1416	9574	4705	26
H(24A)	3881	8105	1410	159
H(24B)	4413	8964	1160	159
H(24C)	3647	8632	563	159
H(25A)	2818	10094	807	194
H(25B)	3666	10393	1303	194
H(25C)	2762	10388	1779	194
H(26)	2405	9234	2513	61
H(27A)	237	5410	897	136

H(27B)	378	5983	1736	136
H(27C)	883	5078	1619	136
H(28A)	2335	6877	1099	95
H(28B)	2225	6184	1852	95
H(28C)	1586	7001	1779	95
H(29)	1925	6318	-132	58
H(30A)	4463	3308	4682	167
H(30B)	3935	4110	4287	167
H(30C)	3483	3177	4405	167
H(31A)	3995	5087	5534	85
H(31B)	4684	4419	5920	85
H(31C)	3835	4650	6442	85
H(32)	2826	3630	6401	59

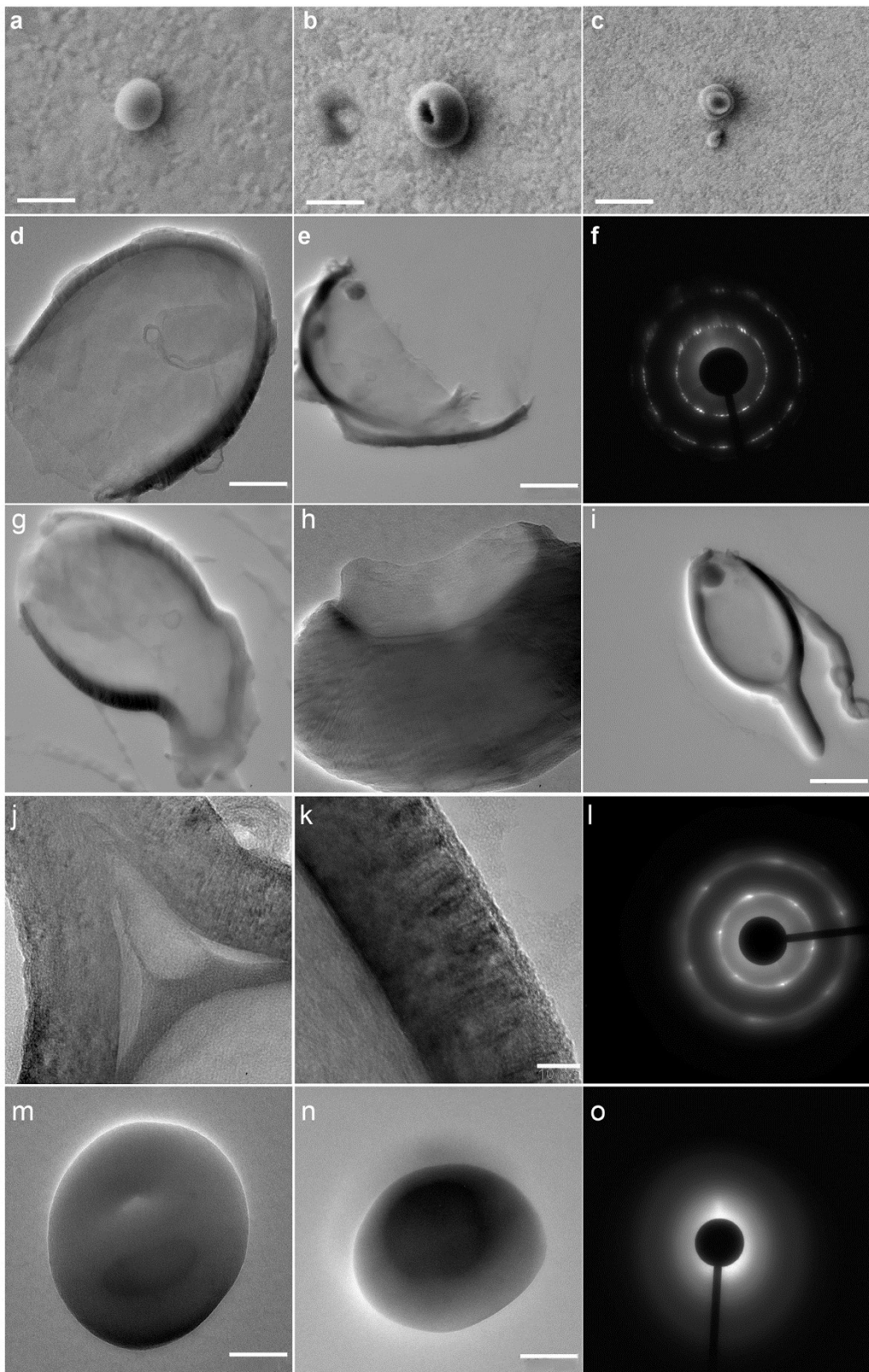


Fig. S14. c-HCS obtained from **2**. **a,b,c**, SEM images of c-HCSs. Scale bars are 0.2, 0.2 and 0.5 μm . **d-i**, TEM images of c-HCSs with electron diffraction from the whole demonstrating their crystallinity. Scale bars, 100 nm (**d-g**), 50 nm (**h**), and 200 nm (**i**). **j-l**, TEM image of c-HCS

from **i**, its shell and electron diffraction from the whole structure. The interlayer period is 3.2 ± 0.3 Å. Scale bars, 20 and 10 nm, respectively. **m-o**, TEM images of amorphous nanoparticles. Scale bar, 50 nm.

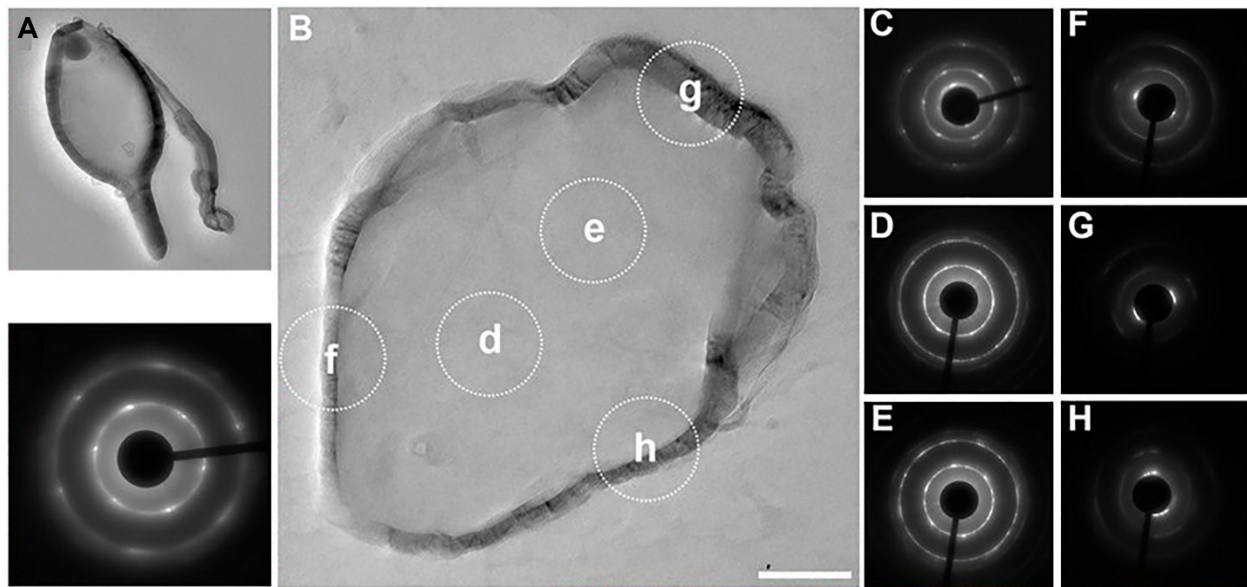


Fig. S15. **(A)** TEM image (top) and the electron diffraction (bottom) from two 80-nm areas near the center of the hemisphere c-HCS. Scale bar, 200 nm. **(B)** TEM image of the hollow c-HCS obtained from **1** demonstrating its crystalline structure by electron diffraction from the whole c-HCS, **(C)**. Scale bar, 50 nm. **(D and E)** Electron diffraction from two 80-nm areas near the center of the c-HCS (**D** and **E**), and **(F to H)** electron diffraction from three 80-nm areas in its shell (**F** to **H**). Scale bar, 50 nm. Pronounced reflexes from each c-HCS indicate the crystallinity of the structures obtained.

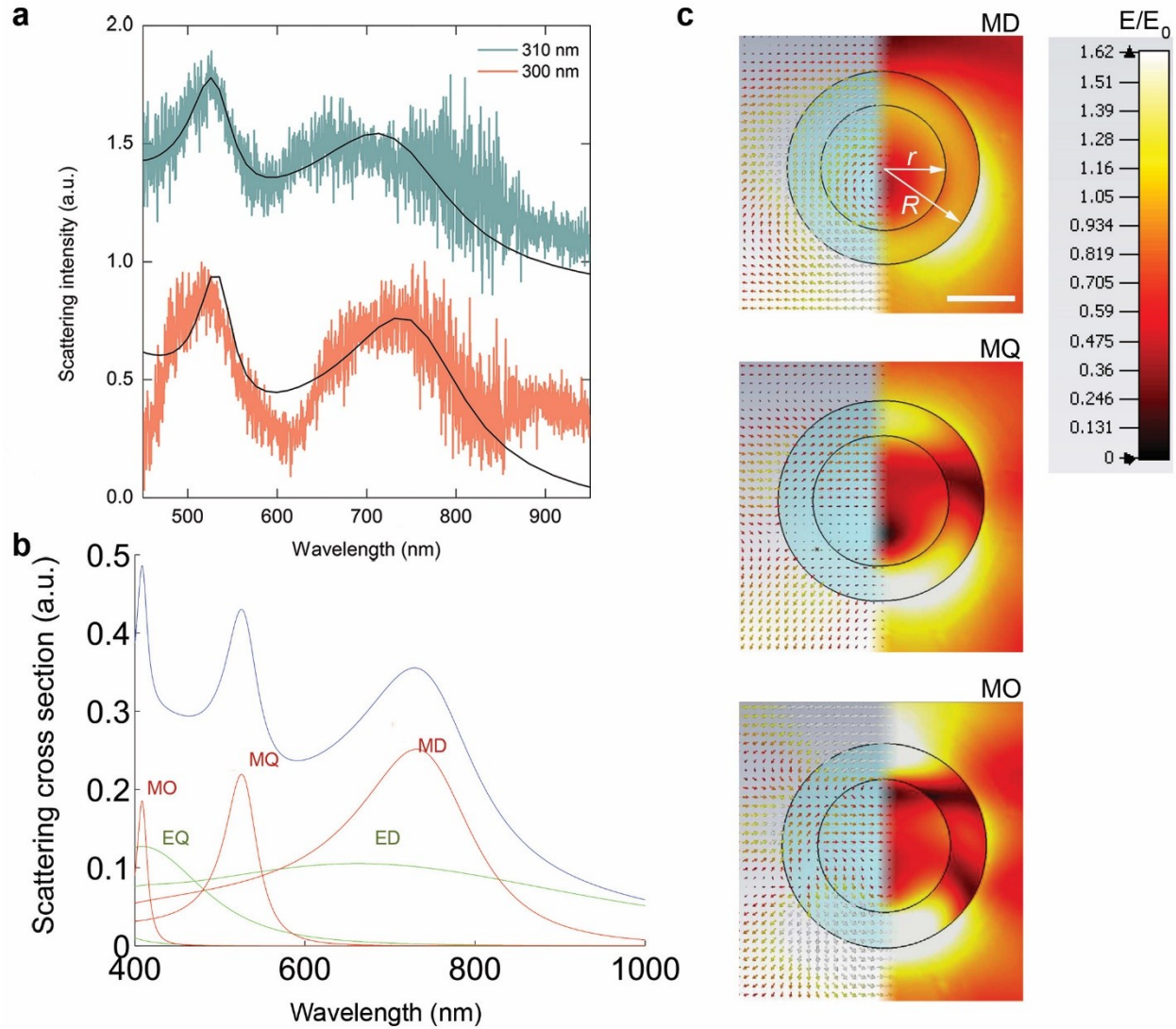


Fig. S16. Modeling for dark field scattering spectra of c-HCS (Fig. 3H). **(a)** Experimental and modeling spectra. **(b)** Contribution of different Mie resonances to the total scattering spectrum of c-HCS with a refractive index of 2.3, radius of 150 nm and shell thickness of 53 nm onto a fused silica (ED – electric dipole, EQ – electric quadrupole, MD – magnetic dipole, MQ – magnetic quadrupole, MO – magnetic octupole), and **(c)** corresponding electromagnetic field distribution inside. R radius of c-HCS, fixed ratio for void radius r ($r/R = 0.65$). The electric field of Mie-type modes is localized inside the shell, while the magnetic part is mostly localized in the cavity of c-HCS. Scale bar, 100 nm.